

International Journal of Modern Physics A  
 © World Scientific Publishing Company

## QCD Phases in Lattice QCD

Sinya AOKI

*Graduate School of Pure and Applied Sciences, University of Tsukuba, Tsukuba,  
 Ibaraki 305-8571, Japan, email: saoki@het.ph.tsukuba.ac.jp and  
 Riken BNL Research Center, Brookhaven National Laboratory, Upton, NY11973, USA*

I review the recent status of lattice QCD calculations at non-zero density.

*Keywords:* Lattice QCD; finite density; critical endpoint; reweighting

### 1. Introduction

It is believed that QCD undergoes phase transitions as temperature  $T$  and the baryon density, controlled by a chemical potential  $\mu$ , increase. For example, an expected phase structure is found in Fig.1 of ref. 1. To theoretically investigate what really happens at non-zero  $T$  and  $\mu$  in QCD, lattice calculations seem ideal. Indeed, as reviewed in ref. 2, lattice QCD investigations are very successful at finite  $T$  but  $\mu = 0$ . On the other hand, lattice QCD simulations at non-zero  $\mu$  have remained to be extremely difficult for a long time, since a complex nature of the lattice QCD action in this case makes a direct application of straightforward Monte-Carlo methods impossible. Recently, however, several new techniques have been proposed to overcome this difficulty and some of them give promising results. In this talk I mainly review recent progresses in lattice QCD at non-zero  $\mu$ .

### 2. Lattice QCD at non-zero $\mu$

A possible solution to the complex action problem at non-zero  $\mu$  was proposed in ref. 3, where a reweighting method from  $\mu = 0$  was employed. This method, called the Glasgow method, however failed since an overlap between gauge ensembles at  $\mu = 0$  and at  $\mu \neq 0$  is exponentially small in the volume.

Recently two new methods have been proposed for small  $\mu$  near the critical temperature  $T_c$ . One is a variant of the Glasgow method: Instead of reweighting only  $\mu$  from  $\mu = 0$ , a multi-parameter reweighting in both  $\mu$  and  $T$  from  $\mu = 0$  and  $T = T_c(\mu = 0)$  is employed<sup>4,5,6,7</sup>. The other method has employed an imaginary chemical potential  $\mu = i\mu_I$  to avoid the complex action problem<sup>8,9</sup>, and then has made an analytic continuation of results to the real  $\mu$  using a Taylor expansion in  $\mu^2$ . Calculations in both methods so far are restricted to  $N_t = 4$ , where the temperature is given by  $T = 1/(N_t a)$ .

2 *Sinya Aoki*

### 2.1. Multi-parameter reweighting method

I first discuss the multi-parameter reweighting method, in which the QCD partition function at non-zero  $\mu$  is rewritten as

$$Z(\beta, \mu, m) = \int \mathcal{D}U \exp[-S_G(\beta, U)] \det D(U, \mu, m) \quad (1)$$

$$= \int \mathcal{D}U \exp[-S_G(\beta', U)] \det D(U, \mu', m) \times \left\{ \exp[-S_G(\beta, U) + S_G(\beta', U)] \frac{\det D(U, \mu, m)}{\det D(U, \mu', m)} \right\} \quad (2)$$

where  $U$  represents a gauge configuration,  $\beta = 6/g^2$  is a inverse of the gauge coupling  $g^2$ ,  $m$  is a quark mass and  $\mu$  is a (quark) chemical potential. Here  $S_G$  is a gauge action and  $\det D$  is a quark determinant. In the actual calculation, gauge configurations are generated at  $\mu' = 0$  and  $\beta' \simeq \beta_c(m, 0)$ , where  $\beta_c(m, \mu)$  is a critical coupling at  $\mu$  and  $m$ . Since both  $\beta$  and  $\mu$  are used in the reweighting, this method is called a multi-parameter reweighting. Once configurations are generated at  $\mu'$  and  $\beta'$ , one can treat the term in  $\{\dots\}$  as a part of observables.

Fodor and Katz<sup>6</sup> have employed the multi-parameter reweighting method starting from gauge configurations generated by 2+1 flavor KS quark action with the plaquette gauge action at  $\mu' = 0$  and  $\beta' = \beta_c$ . Since they have exactly evaluated  $\det D(U, \mu, m)$  appeared in the reweighting factor, lattice volumes in their calculations are restricted to  $L_s^3 \times 4$  with  $L_s = 6, 8, 10, 12$ . Dynamical quark masses in the simulation are

$$\frac{m_{ud}}{T} = 0.0368 \rightarrow \frac{m_\pi}{m_\rho} = 0.188(1), \quad \frac{m_s}{T} = 1.0 \rightarrow \frac{m_\pi}{m_K} = 0.267(1), \quad (3)$$

which are very close to experimental values,  $m_\pi/m_\rho = 0.179$  and  $m_\pi/m_K = 0.267$ .

In order to distinguish the first order phase transition from the crossover, they investigated a volume dependence of Lee-Yang zeros<sup>10</sup>  $\beta_0$ , which are zeros of the partition function  $Z(\beta, \mu, m)$  in the complex  $\beta$  plane. Since there is no real phase transition in the finite volume,  $\text{Im} \beta_0 \neq 0$  at  $V = L_s^3 \neq \infty$ . If  $\lim_{V \rightarrow \infty} \text{Im} \beta_0 = 0$ , there exists the first order phase transition at  $\beta = \beta_0$ , while if  $\lim_{V \rightarrow \infty} \text{Im} \beta_0 \neq 0$ , only a crossover appears at  $\beta = \text{Re} \beta_0$ . In the left of Fig.1, taken from ref. 6,  $\text{Im} \beta_0^\infty$ , obtained by extrapolating  $\beta_0$  to the infinite volume as  $\beta_0(V) = \beta_0^\infty + c/V$ , is shown as a function of  $\mu a$ . The critical endpoint, which separate the first order phase transition line from the crossover line, is estimated to be  $\mu a \simeq 0.18$ . Converting  $(\text{Re} \beta_0^\infty, \mu a)$  to the physical unit  $(T_c, \mu_B = 3\mu)$ , where  $\mu_B$  is a baryonic chemical potential, a phase diagram for QCD at non-zero  $T$  and  $\mu$  is given in the right of Fig.1, also taken from ref. 6, and the critical endpoint becomes  $(T_E, \mu_B^E) = (162(2), 360(40)) \text{ MeV}^6$ .

Instead of evaluating  $\det D(U, \mu, m)$  exactly, Bielefeld-Swansea group has calculated it by the Taylor expansion,

$$\ln \left[ \frac{\det D(U, \mu, m)}{\det D(U, 0, m)} \right] = R_1 \mu + R_2 \mu^2 + \dots, \quad (4)$$

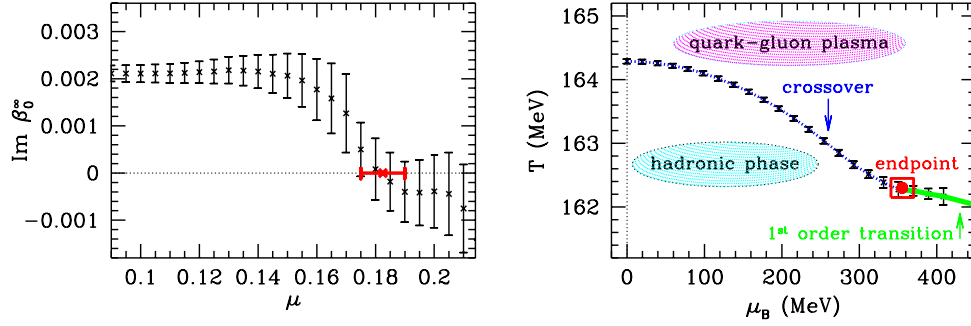


Fig. 1. (Left)  $\text{Im } \beta_0^\infty$  as a function of the chemical potential. (Right) The phase diagram in physical unit.

to perform the simulation on a relatively large volume,  $16^3 \times 4$ . Gauge configurations are generated by the improved gauge action and the  $N_f = 2$  p4-improved KS quark action at  $m/T = 0.4, 0.8$ , corresponded to  $m_\pi/m_\rho \simeq 0.7, 0.85$ . The transition temperature was estimated from the peak position of susceptibilities  $\chi_{\bar{\psi}\psi}$  and  $\chi_L$ , where  $L$  is the Polyakov loop. The result of the critical temperature  $T_c(\mu)$  as function of the quark chemical potential  $\mu_q$  can be found in Fig.16 of ref. 7. Errors of the reweighting remain small at  $\frac{\mu_q}{T} \leq 0.4$ , but they increase as  $\mu_q$  becomes larger.

## 2.2. Imaginary chemical potential

Since the quark determinant  $\det(U, i\mu_I, m)$  becomes real for the imaginary chemical potential  $i\mu_I$ , direct Monte-Carlo simulations are possible in this case<sup>8,9</sup>. One then fits the critical temperature obtained at the imaginary chemical potential in the form of the Taylor expansion:

$$T_c(i\mu_I) = T_c(0) + c_2\mu_I^2 + O(\mu_I^4), \quad (5)$$

as seen in Fig. 9 of ref. 9 for  $N_f = 2$  and in Fig.6 of ref. 8 for  $N_f = 4$ . Assuming an analyticity at  $\mu = 0$ , one immediately obtain the critical temperature at real  $\mu$ :

$$T_c(\mu) = T_c(0) - c_2\mu^2 + O(\mu^4). \quad (6)$$

In this method, a restriction that  $|\bar{\mu}_I \equiv \frac{\mu_I}{T}| \leq \frac{\pi}{3}$  exists, due to periodicity and symmetry, which leads to

$$Z(\bar{\mu}_I = \frac{\pi}{3} + x) = Z(\bar{\mu}_I = \frac{\pi}{3} - x), \quad (7)$$

as explicitly confirmed in Fig.6 of ref. 9.

Table 1. Values of  $C$  from various simulations. Here Imag, MulPar-Rew, MulParRewTay represent the imaginary chemical potential, the multi-parameter reweighting and the multi-parameter reweighting with the Taylor expansion, respectively. The superscript of the method is the reference number.

$N_f$	$C$	$m_{ud}/T$	$m_s/T$	quark	method <sup>ref.</sup>
2	0.0056(4)	0.1	-	KS	Imag <sup>9</sup>
	0.008(3)	0.4, 0.8	-	p4	MulParRewTay <sup>7,11</sup>
2+1	0.0032	0.0368	1.0	KS	MulParRew <sup>6</sup>
3	0.0028(7)	0.4	0.4	p4	MulParRewTay <sup>11</sup>
	0.013(5)	0.02	0.02	p4	MulParRewTay <sup>11</sup>
4	0.011	0.2	-	KS	Imag <sup>8</sup>

### 2.3. Comparison of various results

The critical temperature  $T_c$  can be parameterized as a function of the baryonic chemical potential  $\mu_B$  as

$$\frac{T_c(\mu_B)}{T_c(0)} = 1 - C \frac{\mu_B^2}{T_c(0)^2}. \quad (8)$$

Results for  $C$  from various simulations are accumulated in table 1, which indicates that  $C$  becomes larger as  $N_f$  increases. Further investigations including the quark mass dependence, however, will be required for the definite conclusion on the  $N_f$  dependence of  $C$ .

A critical endpoint  $(\mu_B^E, T_E)$  is a point on the critical temperature line which separates the cross-over from the first order phase transition. Results of the critical endpoint from two groups are given in table 2, from which one may notice that the location of the critical endpoint strongly depends on the quark mass. Again further investigations will be required for the reliable estimate on the location of the critical endpoint for the physical case.

One may convert the mass dependence of the critical endpoint to the  $\mu$  dependence of the critical quark mass as

$$\frac{m_c(\mu_q)}{m_c(0)} = 1 + D \left( \frac{\mu_q}{\pi T_c} \right)^2, \quad (9)$$

where the critical quark mass separates the first order phase transition from the cross-over: the phase transition is the first order at  $m < m_c$  while it becomes cross-over at  $m > m_c$ . For the  $N_f = 3$  case, The imaginary chemical potential method<sup>12</sup>, using the KS quark action, gives  $D = 0.84(36)$  and  $m_c(0)/T = 0.123(1)$ , while the multi-parameter reweighting method with the Taylor expansion<sup>11</sup>, using the p4-improved KS quark action, leads to  $D = 690$  and  $m_c(0)/T = 0.0028(16)$ . Although errors are large and quark actions are different, a discrepancy between two results

Table 2. The critical endpoints  $(\mu_B^E, T_E)$ , together with the critical temperature  $T_c$  at  $\mu_B = 0$ .

$N_f$	$\mu_B^E$ MeV	$T_E$ MeV	$T_c$ MeV	$m_{ud}/T$	$m_s/T$	quark	method <sup>ref.</sup>
2+1	725(35)	160(4)	172(3)	0.1	0.8	KS	Lee-Yang zero <sup>5</sup>
	360(40)	162(2)	164(2)	0.0368	1.0	KS	Lee-Yang zero <sup>6</sup>
3	0	-	-	0.0028(16)	0.0028(16)	p4	Binder cumulants <sup>11</sup>
	156(30)	-	-	0.02	0.02	p4	Binder cumulants <sup>11</sup>

is huge. We will have to understand and resolve this discrepancy, in order to make the definite conclusion for the phase structure at non-zero chemical potential.

### 3. Some remarks

#### 3.1. Reweighting vs. imaginary chemical potential

One can check a reliability of the reweighting method by comparing it with the direct calculation in the case of the imaginary chemical potential. In the left of Fig. 2, taken from ref. 4,  $\langle \bar{\psi}\psi \rangle$  is plotted as a function of  $\mu_I$ . The multi-parameter reweighting method agrees with the direct calculation, while the Glasgow method does not. This comparison may suggest that the multi-parameter reweighting is more reliable. As mentioned in the previous subsection, however, the result must be symmetric in  $\mu_I$  at  $\mu_I = \pi/12 \simeq 0.26$ . This symmetric property is clearly violated in both multi-parameter reweighting method and the direct calculation. It is likely that the violation may be caused by the insufficient statistics for both methods. Therefore, in the case of the reweighting method, one should always check whether the symmetric property is satisfied or not for the imaginary chemical potential, using the same ensemble employed for the reweighting of real  $\mu$ .

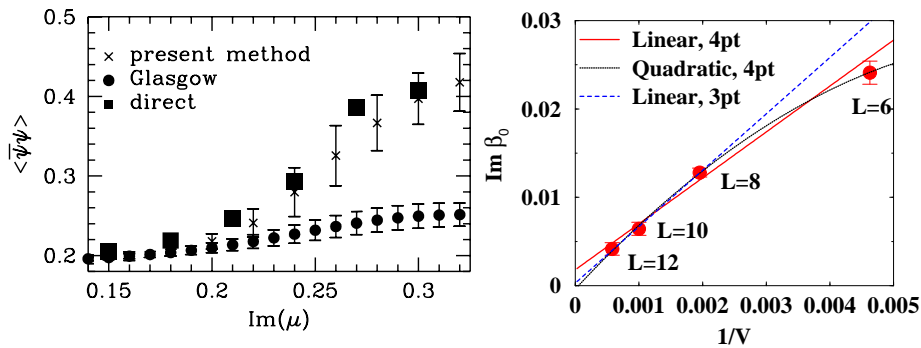


Fig. 2. (Left)  $\langle \bar{\psi}\psi \rangle$  as a function of  $\text{Im} \mu$  for the direct simulation (squares), the multi-parameter reweighting (crosses) and the Glasgow method (circles). (Right)  $\text{Im} \beta_0$  as a function of  $1/V$  at  $\mu a = 0.16$ , together with the linear fit (solid line), the quadratic fit (dotted line) and the linear fit for larger 3 volumes (dashed line).

### 3.2. Cautions to the Lee-Yang zero analysis

It has been pointed out that the partition function becomes zero in the infinite volume limit for all  $\mu \neq 0$ :  $\lim_{V \rightarrow \infty} Z(\mu \neq 0, V) = 0$ , due to the sign problem of the complex action<sup>13</sup>. Therefore one should check the volume dependence of not only the 1st Lee-Yang zero but also the 2nd, 3rd,  $\dots$  Lee-Yang zeros, in order to distinguish the first order phase transition from the cross-over.

In addition to the above subtlety, the procedure of taking  $V \rightarrow \infty$  limit<sup>6</sup> may cause some systematic uncertainties in the estimation of the critical endpoint. For example, an extrapolation linear in  $1/V$  for 4 volumes ( $V = 6^3, 8^3, 10^3, 12^3$ ) gives  $\text{Im } \beta_0^\infty = 0.0018(7)$  at  $\mu a = 0.16$ , suggesting that this point corresponds to the cross-over. As shown in the right of Fig. 2, however, the quadratic fit for 4 volumes or the linear fit for larger 3 volumes gives  $\text{Im } \beta_c^\infty = -0.0004(11)$  or  $0.0003(9)$ , respectively, concluding that the phase transition is consistent with the first order. Clearly a more careful finite volume analysis is required for a definite conclusion on the location of the critical endpoint at non-zero  $\mu$ .

## 4. Conclusions

By recent developments for lattice QCD techniques, numerical simulations become possible at small  $\mu$  and non-zero  $T$ . Preliminary results suggest  $\mu_B^E \simeq 350 - 450$  MeV at physical light and strange quark masses. However further confirmations will be definitely required for the reliable estimate of  $\mu_B^E$ . So far numerical simulations at non-zero  $\mu$  have been performed only with KS fermions. Therefore new calculations by other fermion formulations such as Wilson/clover or domain-wall/overlap fermions will be necessary to check the present results by KS fermions. Definitely new ideas will be needed to explore QCD phase structure at large  $\mu$  and low  $T$ .

## Acknowledgments

This work is supported in part by the Grant-in-Aid of the Ministry of Education (Nos. 13135204, 15540251, 16028201).

## References

1. S. Hands, *Nucl. Phys. B (Proc. Suppl.)* **106& 107**, 142 (2002).
2. S. Ejiri, *Nucl. Phys. B (Proc. Suppl.)* **94**, 19 (2001).
3. I.M. Barbour and A.J. Bell, *Nucl. Phys. B* **372** 385 (1992); I.M. Barbour *et al.*, *Nucl. Phys. B (Proc. Suppl.)* **60A** 220 (1998).
4. Z. Fodor and S.D. Katz, *Phys. Lett. B* **534**, 87 (2002).
5. Z. Fodor and S.D. Katz, *JHEP* **0203**, 014 (2002).
6. Z. Fodor and S.D. Katz, *JHEP* **0404**, 050 (2004).
7. C.R. Alton *et al.*, *Phys. Rev. D* **66**, 074507 (2002).
8. M. D'Elia and M-P. Lombardo, *Phys. Rev. D* **67**, 014505 (2003).
9. P. de Forcrand and O. Philipsen, *Nucl. Phys. B* **642**, 290 (2002).
10. C. N. Yang and T. D. Lee, *Phys. Rev.* **87**, 404 (1952).

11. S. Ejiri *et al.*, *Prog. Theor. Phys. Suppl.* **153**, 118 (2004); F. Karsch *et al.*, *Nucl. Phys.* **B(Proc. Suppl.)129**, 614 (2004).
12. P. de Forcrand and O. Philipsen, *Nucl. Phys.* **B673**, 170 (2003).
13. S. Ejiri, *Phys. Rev.* **D69**, 094506 (2004).